Flight Effects on JT8D Engine Jet Noise Measured in a 40 × 80 Tunnel

Frank G. Strout*
Boeing Commercial Airplane Company, Seattle, Wash.
and
Adolph Atencio Jr.†
NASA Ames Directorate, Moffett Field, Calif.

A JT8D-17 turbofan engine was tested in the NASA Ames Reserach Center 40 × 80 ft wind tunnel to determine flight effects on jet noise. The engine was configured as a baseline with conical nozzle, a quiet-nacelle 20-lobe ejector/suppressor, and an internal mixer with conical nozzle. Tunnel-off and tunnel-on noise tests were conducted over a range of nozzle pressure ratios (1.2 to 2.1), primary jet velocities (275 to 550 m/sec), and tunnel velocities up to 100 m/sec. Aft quadrant noise data were measured by a pair of traversing microphones located on a 3-m sideline relative to the engine centerline. Unique correlations and analysis procedures were developed in order to define far-field flight effects from the relatively near-field noise measurements. Wind-tunnel-derived flight effects compare favorably with 727/JT8D flight-test data and model data obtained in a smaller wind tunnel for both the baseline and 20-lobe ejector/suppressor configurations. The study shows the importance of testing suppressor concepts for flight noise. It was found that the ejector/suppressor experienced a significant loss of suppression relative to static measurements during flight, whereas the internal mixer indicated a slight gain in suppression. It is concluded that the wind tunnel is a viable method for studying flight effects on engine jet noise.

Nomenclature

D	= diameter, m
ej/supp	= ejector/suppressor
mic	= microphone
n	= velocity index
NPR	= nozzle pressure ratio
OB	= octave band
V_{ej}	= ejector exit velocity, m/sec
V_j	= jet velocity, m/sec
V_{mix}	= jet velocity of mixed fan and primary flows, m/sec
V_{pint}	= ejector internal primary velocity, m/sec
V_{pri}	= engine primary jet velocity, m/sec
V_R	= relative jet velocity = $V - V_\infty$, m/sec
V_{rej}	= ejector exit relative velocity = $V_{ej} - V_\infty$, m/sec
V_{sec}	= velocity of entrained ejector air, m/sec
V_T	= nominal tunnel test velocity, m/sec
V_∞	= aircraft or tunnel velocity, m/sec
X_s	= source location along jet axis, m
θ_F	= far-field angle
θ_N	= near-field angle
∞	= ambient

Introduction

THERE is currently an industry-wide interest in understanding and defining the influence of flight on aircraft engine noise. The need for accurate flight effects will increase as the requirements for efficient, low-noise aircraft become more demanding. Engine noise-reduction concepts typically are developed on static-test facilities. These quiet systems must be designed for peak effectiveness during flight, which in turn requires a precise definition of static-to-flight noise changes. The most direct method of obtaining this knowledge is to compare static and flight-test data that have been corrected to a common base. The use of flight test during engine system development phases and for detailed noise research has limitations in terms of experiment control, accuracy, and cost. Accordingly, industry is pursuing a number of flight simulation techniques that may be used to study and define accurately flight effects on engine noise in a cost-effective manner.

This paper summarizes the results of a noise test conducted in the NASA Ames Research Center (ARC) 40 × 80 ft wind tunnel with a JT8D-17 turbofan engine provided by Pratt and Whitney Aircraft Corporation. The test and analysis techniques were developed previously by Boeing during model tests conducted in a smaller wind-tunnel facility. The full-scale test results and findings are presented in Ref. 1, which was prepared in compliance with NASA ARC Contract NAS 2-8213. The major objectives of the program were to: 1) determine feasibility of wind-tunnel tests for studying flight effects; 2) establish flight effects on jet noise for the JT8D engine configured as a baseline, 20-lobe ejector/suppressor, and internal mixer; and 3) compare 40 × 80 ft wind-tunnel-derived flight effects with available 727/JT8D flight-test results and Boeing 9 × 9 ft wind-tunnel model test results.

Test Description

The test was conducted in the NASA ARC 40 × 80 ft wind tunnel. The test engine was a JT8D-17 turbofan engine, provided by Pratt and Whitney Aircraft Corporation. The engine develops a thrust of approximately 71 kN (16,000 lb) at an engine pressure ratio of 2.2 and has a bypass ratio of 1.1.

Three major configurations were tested including a baseline, a quiet-nacelle 20-lobe ejector/suppressor, and an internal mixer. All three configurations were tested with the quiet-nacelle two-ring inlet in order to minimize inlet fan noise. The fan and primary streams of the baseline configuration merge internally and exhaust through a common conical nozzle that is 0.76 m (2.5 ft) in diameter. The outer fan flow is partially mixed with the primary flow at the nozzle exit. For this configuration, the jet noise is dominated by the high-velocity primary flow.

Presented as Paper 76-556 at the 3rd AIAA Aero-Acoustics Conference, Palo Alto, Calif., July 20-23, 1976; submitted July 28, 1976; revision received Dec. 17, 1976.
Index category: Noise.

*Noise Research Engineer, Noise Technology Staff.
†Research Engineer, U.S. Army Air Mobility Research and Development Laboratory.

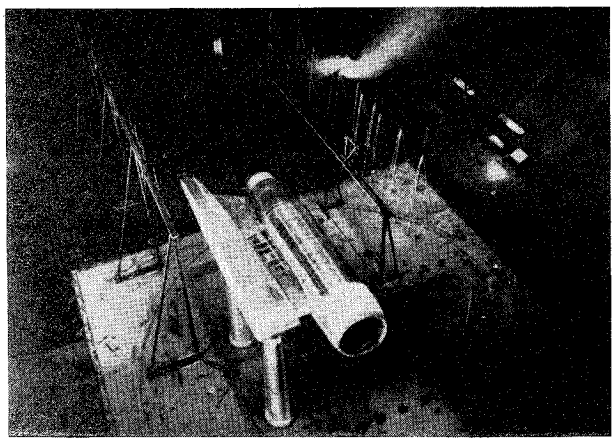

Fig. 1 Test installation, JT8D-17 in NASA Ames Research Center 40- × 80-ft wind tunnel.

The 20-lobe ejector/suppressor directs the fan and primary flow streams into 20 discrete lobes that are spaced uniformly around a plug. Tertiary air is entrained through eight blow-in doors, where it mixes with the fan and primary jets. An acoustically lined ejector shroud, having an area ratio of 1.8, surrounds the 20-lobe nozzle. The exhaust flow at the ejector exit is relatively well mixed. The dominant jet noise for this configuration is generated within the ejector by the mixing process between the entrained tertiary air and the discrete primary jets.

The internal mixer incorporates a 12-lobe device that promotes rapid internal mixing of the fan and primary flows. The streams are reasonably well mixed and are exhausted through a common conical nozzle having a diameter essentially the same as the baseline. The mixed jet velocity is substantially less than the baseline primary velocity and results in a reduced jet noise level.

The side-mounted baseline configuration and acoustic instrumentation are shown in Fig. 1. Noise measurements were made by a pair of beam-mounted traversing microphones that were used to record data in steady-state mode at discrete angles and in sweep mode. The data from the fixed microphone arrays were used as backup information. The microphones were located on a 3-m (10-ft) sideline and covered aft quadrant angles from 90° to 165°. Engine, nozzle, and facility parameters were measured and recorded in order to monitor engine operation and performance (thrust and jet velocities), ejector performance, and tunnel velocity. Tunnel-off and tunnel-on noise tests were conducted over a range of nozzle pressure ratios (1.2 to 2.1), primary jet velocities (275 to 550 m/sec), and tunnel velocities up to 100 m/sec. Acoustic data were recorded on 14-track analog tape and were reduced to provide tabulated and plotted ⅓-octave-band (OB) spectra.

Wind-Tunnel Data-Analysis Technique

The noise measurements in the 40 × 80 ft wind tunnel were made relatively close to the engine noise sources. The sideline distance was selected to minimize reverberant field effects while at the same time avoiding dominant near-field effects. Ideally, measurements would be taken in the acoustic far field, where noise source locations are relatively unimportant to data analysis. At the test-measuring station of 3 m, however, noise source location and directivity are very important to a proper evaluation of the acoustic data.

For noise sources that originate at or very near the engine exit plane (core noise, suppressor premerged mixing noise), the near- and far-field signals are common and will differ in level primarily due to propagation distance and atmospheric absorption. Wind-tunnel flight effects analysis of this data is based on near-field tunnel-off to tunnel-on noise increments being equal to far-field noise increments at equal angles referenced to the engine exit.

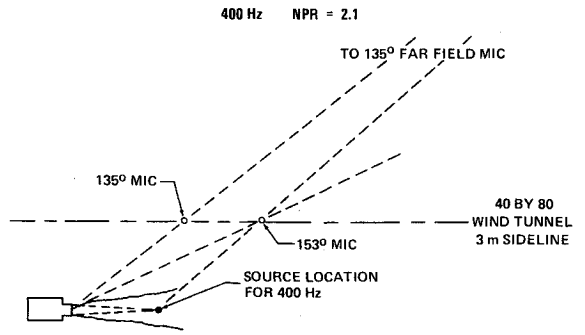

Fig. 2 Wind-tunnel flight effects analysis, near-/far-field angle relationship.

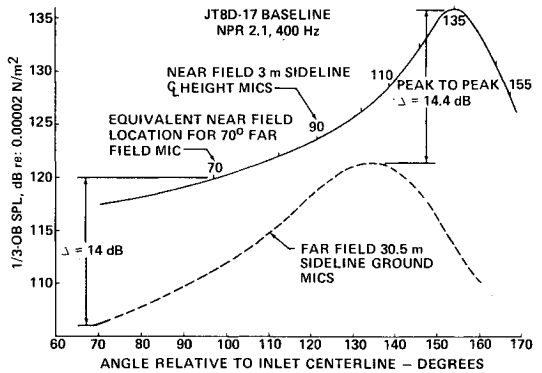

Fig. 3 Typical near- and far-field SPL directivity comparison.

Noise generated by the jet as it mixes with surrounding ambient air presents a more difficult problem. The proximity of the near-field microphones to the sources requires that source location and directivity be known for each frequency of interest if accurate far-field flight effects are to be identified. This is illustrated in Fig. 2, where the geometric relationship for a 400-Hz signal is defined. The angles originate at the nozzle exit plane center and are referenced to the inlet axis. The signal in propagating to a far-field station (135°) will pass through a near-field station having a larger geometric angle (153°). The far-field flight effect for this frequency will be measured at a near-field angle of 153° rather than 135°. A method of defining approximate source location and directivities has been devised involving the use of multiple sideline data recordings. The analysis is based on the premise that spherical divergence and atmospheric absorption account for the level differences observed for a given signal as it passes from a source location through a given near-field location to the far-field location.

Data recorded for the JT8D-17 engine at a static-test facility were used to establish the necessary near- to far-field correlations. Near-field (3-m sideline, centerline mic's) and far-field (30.5-m, ground mic's) SPL's are plotted vs angle for a given ⅓-OB frequency, as shown in Fig. 3. The peak-to-peak difference is 14.4 dB. This is approximately correct to account for spherical divergence (+20 dB), differences in level relative to free field (about −5 dB), and atmospheric absorption. Assuming that the peak-to-peak SPL difference is valid at all emission angles, each far-field angle is related to a near-field angle as shown in Fig. 3. A curve then is plotted which relates the far- and near-field angle for each frequency as shown in Fig. 4. The final plots were faired through the bulk of data, with the heaviest weighting placed on the near/far peak noise relationship for each frequency. Correlations similar to Fig. 4 were defined for each test configuration at several engine power settings. The measured change in noise at a given near-field angle, due to tunnel flow, is equated to the far-field noise change at an angle defined by the appropriate correlation.

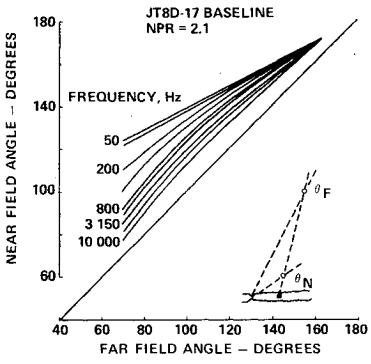

Fig. 4 Near-/far-field correlation for frequencies.

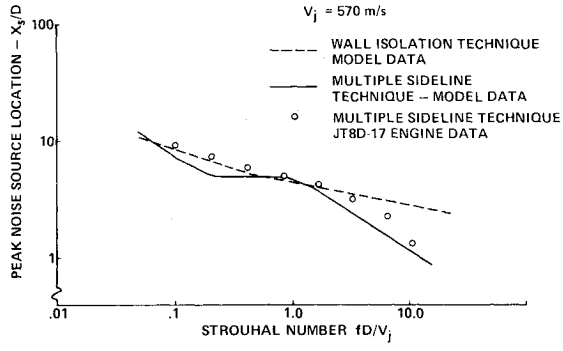

Fig. 5 Comparison of peak noise source location.

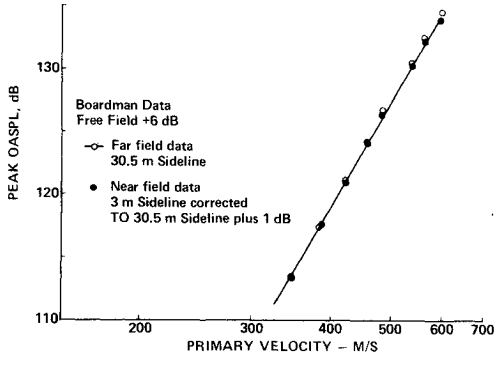

Fig. 6 Comparison of near- and far-field peak OASPL vs jet velocity for baseline JT8D engine.

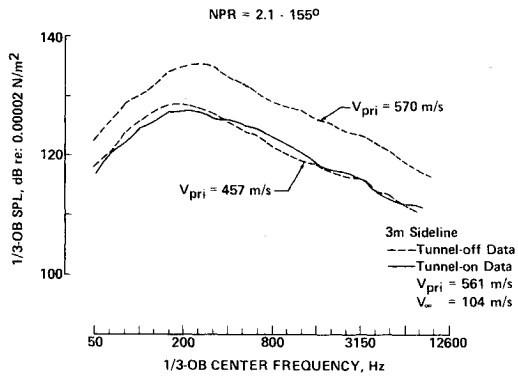

Fig. 7 JT8D-17 engine, baseline static/flight spectra.

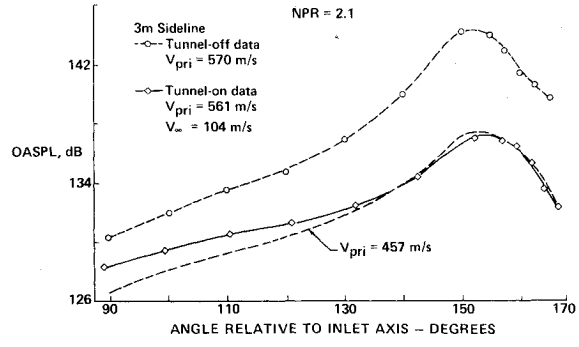

Fig. 8 JT8D-17 engine, baseline static/flight OASPL directivity.

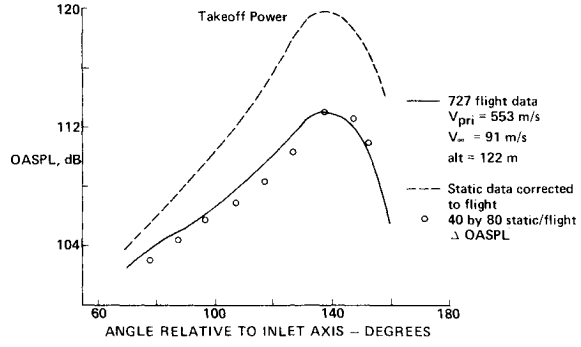

Fig. 9 JT8D engine, baseline static/flight OASPL directivity: 40 × 80 vs 727 flight data.

The near-/far-field angle correlations define an apparent source location along the jet for each frequency and each far-field angle. The resulting peak noise source location for frequencies from 50 to 10,000 Hz are compared with similar data obtained using model jets in Fig. 5. The wall isolation technique[2] and a correlation using three sidelines show source locations that are in reasonable agreement with those defined for the full-scale engine.

Verification of the correlations and analysis technique requires comparisons of wind-tunnel and flight-test results. This is done for the baseline and 20-lobe ejector/suppressor in the following sections. Another check on the significance of near-field measurements is provided by comparing peak near- and far-field static noise levels as a function of primary jet velocity. Near- and far-field peak noise levels for the baseline configuration are compared in Fig. 6, where near-field data have been extrapolated to the far-field sideline by applying spherical divergence and atmospheric attenuation corrections. As indicated, the extrapolated near-field peak OASPL's are about the same level as the far-field values and have the same slope with jet velocity. Comparable results are indicated for discrete frequencies from 63 to 10,000 Hz. Thus, under static conditions as engine power is varied, a change in peak near-field noise is the same as that in the far field. These comparisons do not necessarily validate the near- to far-field correlations. They do provide confidence that noise measured relatively near the sources can be extrapolated and interpreted to define meaningful far-field noise characteristics, at least for peak noise. Near-field effects also are judged to be relatively minor on the basis of these comparisons. During tunnel-on operation, engine noise is convected downstream by the moving medium. A convection correlation is applied so that tunnel-off and tunnel-on noise data are compared at equal emission angles.

Baseline Results

Typical tunnel-off and tunnel-on spectra are provided in Fig. 7 for the baseline configuration at takeoff power. The spectra for the near-field angle shown are approximately equivalent to far-field spectra at an angle of 140° (peak noise) based on the near-/far-field correlations. The measured tunnel-on data are representative of flight, with the exception of Doppler frequency shift, which occurs as a moving source passes an observer. To correct for this, the spectra have been shifted to a lower frequency by about a third-octave band.

A reference spectrum is included which represents interpolated tunnel-off data at the tunnel-on relative velocity ($V_{pri} - V_{\infty}$). As indicated, the tunnel-on spectra compare reasonably well with the reference spectra. This indicates that a good estimate of peak flight noise can be made by interpolating static data at flight primary relative velocity.

Tunnel-off and tunnel-on OASPL directivities are compared in Fig. 8 for the takeoff power condition. Reference curves also are included which represent interpolated tunnel-off data at tunnel-on primary relative velocity. The comparisons show that the largest reduction of noise due to tunnel flow occurs at or near peak noise location. The low-angle reduction is significantly less, whereas the higher angles show slightly less reduction than the reduction at peak noise. The peak noise location is approximately the same for both tunnel-off and tunnel-on.

The tunnel-on (flight) OASPL's are approximated closely by the reference relative velocity noise level at angles of 140° and higher. Lower angles show less flight noise reduction than predicted by relative velocity. Note that these are near-field angles where the 155° peak noise location is equivalent to a far-field angle of about 140°, whereas 110° is equivalent to a far-field angle of approximately 90°.

Comparison of Wind-Tunnel and 727 Flight Data: Baseline Nozzle

The 727 flight test was conducted previously with JT8D-9 engines, where 122-m (400-ft) level flyover noise data were recorded using ground microphones.[3] The jet noise characteristics of the -9 and -17 engines are essentially the same for a given jet velocity. The flight data are the average of three flyovers and three ground microphone recordings. Wind-tunnel and static-test data that are extrapolated to the flight conditions are corrected for slight differences in engine power, three-engine operation, angle of attack (6°), and noise source location. Two techniques are used to compare 40- × 80-ft wind-tunnel test results for the baseline with the flight-test results. One technique is based on measured tunnel-off to tunnel-on noise increments. The second approach relies on extrapolating the absolute tunnel-on noise levels to the flight condition. The directivity comparison of Fig. 9 is based on the noise increment procedure and reflects takeoff power.

The reference static noise level is extrapolated far-field data and indicates the amount of noise reduction which occurs due to flight at each angle. The reduction of noise is substantial at angles near peak (140°) but is relatively small at low angles (70°). The wind-tunnel flight noise is established by subtracting the measured tunnel-off to tunnel-on noise increments from the reference static noise level. The increments were obtained from Fig. 8. The resulting comparison shows good agreement in terms of flight noise level and directivity.

Absolute tunnel-on noise levels are extrapolated to the flight condition and compared with flight-test results in Fig. 10. The tunnel-on condition was selected to match the flight parameters. The data are extrapolated by applying spherical divergence and standard day atmospheric absorption to the proper noise emission angle. This comparison also shows good agreement between the wind-tunnel and flight-test OASPL values. Another means of comparing wind-tunnel and flight-test noise characteristics is illustrated in Fig. 11, where velocity index values are plotted. As indicated, velocity index values compare well in terms of absolute level and trend with angle.

Baseline Model Results

A 1/7-scale model of the JT8D baseline was tested in the Boeing 9 × 9 ft wind tunnel. The facility uses a traversing microphone and includes acoustically lined walls in the test section to minimize reverberation. The model was supplied with heated dual flow at conditions equivalent to the JT8D-17 cycle. Tunnel-off and tunnel-on OASPL directivities are shown in Fig. 12 for takeoff power. The model-scale results are similar to the full-scale wind-tunnel test results in showing a flight noise reduction approximately equal to the relative velocity reference level at angles above 140°, with less reduction at low angles.

20-Lobe Ejector/Suppressor Nozzle

Tunnel-off and tunnel-on spectra are shown in Fig. 13 for the 20-lobe ejector/suppressor configuration at takeoff power. The spectra for the listed near-field angle are representative of far-field spectra at the same angle. The noise signal to low angles through peak (120°) is dominated by premerged mixing noise (200 to 3150 Hz). This noise component is generated by the discrete primary and tertiary air-mixing process within the ejector and radiates a common signal to the near and far fields. The postmerged jet noise is generated by the mixing between the ejector exhaust and the freestream. This component becomes more dominant at angles near the jet axis, where a near- to far-field angular adjustment is required to evaluate wind-tunnel flight effects properly.

A reference spectrum is included in Fig. 13 which represents tunnel-off data at the tunnel-on primary relative velocity. The tunnel-on spectra at 120° have been adjusted slightly to account for Doppler frequency shift. As indicated, the premerged mixing noise undergoes a small level reduction due

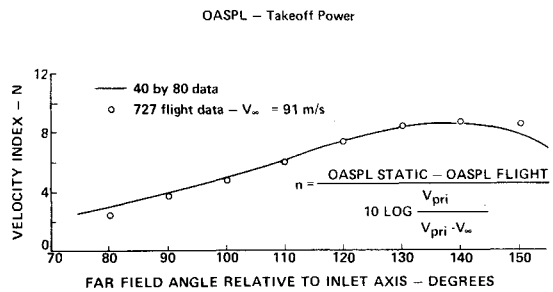

Fig. 11 JT8D engine, baseline relative velocity index comparison: 40 × 80 vs flight data.

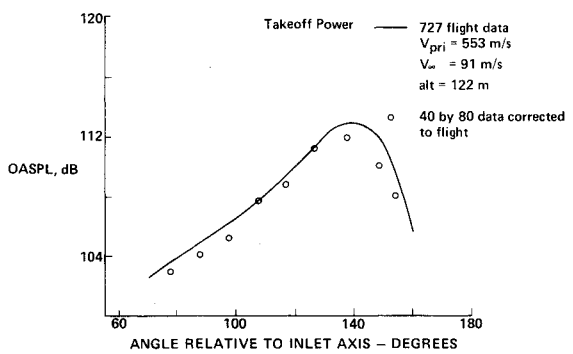

Fig. 10 JT8D engine, baseline flight OASPL directivity: 40 × 80 vs 727 flight data.

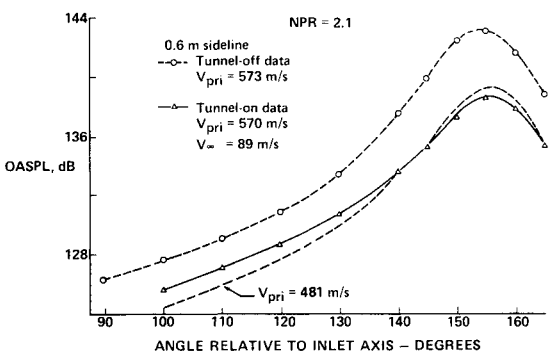

Fig. 12 JT8D baseline model static/flight OASPL directivity.

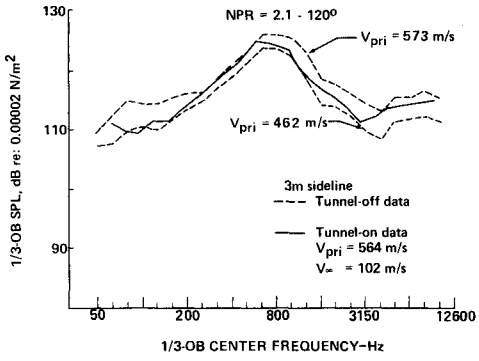

Fig. 13 JT8D-17 baseline model static/flight OASPL directivity.

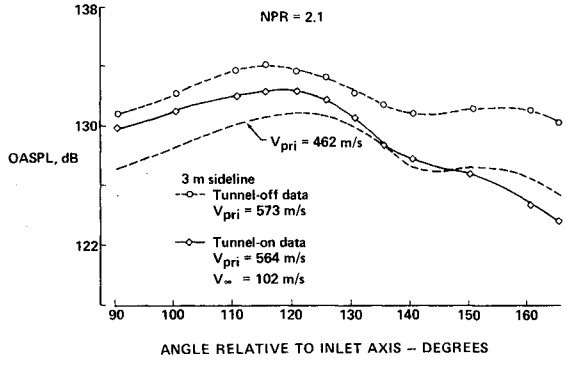

Fig. 14 JT8D-17 engine, 20-lobe ejector/suppressor static/flight OASPL directivity.

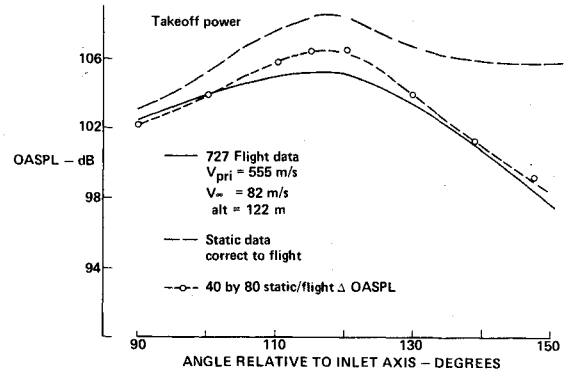

Fig. 15 JT8D engine, 20-lobe ejector/suppressor static/flight OASPL directivity: 40 × 80 vs 727 flight data.

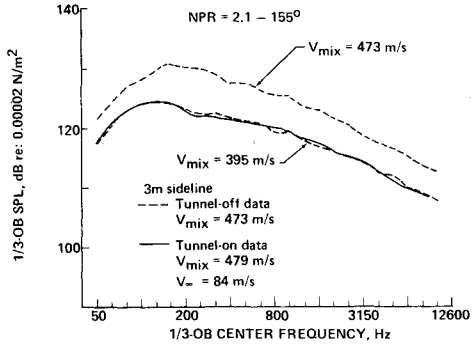

Fig. 16 JT8D-17 engine, internal mixer static/flight spectra.

to tunnel flow. Ejector flow parameters measured during the test show that the internal relative velocity ($V_{Pint} - V_{sec}$) decreases only slightly with tunnel velocity. This results in a correspondingly small decrease in the important premerged mixing noise with tunnel flow. The low-frequency noise (50-125 Hz) experiences a larger reduction due to tunnel flow. This noise is dominated by the postmerged mixing process, which experiences a relative velocity type of reduction with forward velocity. The amount of low-frequency noise reduction increases as the jet axis is approached.

Tunnel-off and tunnel-on OASPL directivities are compared in Fig. 14 for takeoff power. A reference noise level is included which represents tunnel-off data at a primary jet velocity equal to the tunnel-on primary relative velocity. The OASPL comparison indicates relatively small reductions of noise due to tunnel flow at low angles through peak noise, with larger reductions occurring at angles near the jet axis. With the amount of noise reduction greater at higher angles, there is a natural tendency for the in-flight peak noise to shift toward the inlet axis. For this power setting, however, the change in peak noise location due to flight is slight.

The small reduction of OASPL at low angles is the result of premerged mixing noise dominance in this region. The premerged noise, generated within the ejector, undergoes a small reduction due to flight; consequently, OASPL is reduced by a small amount. At angles near the jet axis, the postmerged mixing noise is more dominant. This component undergoes a relative velocity type of reduction with forward velocity; thus OASPL is reduced substantially.

The reference relative velocity noise level overpredicts the amount of low and peak angle noise reduction and underpredicts the reduction at angles near the jet axis. The reference level is based on the relative velocity of the primary jet. This does not fit the noise-generating mechanism of either the premerged or postmerged mixing process and results in a poor prediction of in-flight noise at most angles.

Comparison of Wind-Tunnel and 727 Flight Data: 20-Lobe Ejector/Suppressor Nozzle

The 727 was flight-tested previously with 20-lobe ejector/suppressors installed on each engine.[3] Wind-tunnel and static-test data are extrapolated to the flight condition in the manner described for the baseline. It is noted that wind-tunnel data at angles from 90° to 120° are related to the far-field flight data on an equal angle basis, whereas higher angles employ a near- to far-field correlation. Wind-tunnel and 727 flight OASPL directivities for the 20-lobe ejector/suppressor are compared in Fig. 15 at takeoff power. The wind-tunnel noise levels are based on measured tunnel-off to tunnel-on increments that are applied to extrapolated far-field static data. In general, the wind-tunnel and flight-test noise levels compare favorably. Both the wind-tunnel and flight data indicate a small reduction of OASPL due to flight at low angles (90°). The amount of reduction increases as the angle increases toward the jet axis. The wind tunnel indicates slightly less reduction of peak OASPL by about 1 dB. Absolute tunnel-on noise levels extrapolated to the flight condition also compare well with flight data. On the basis of wind-tunnel and flight-test directivity comparisons for both the baseline and 20-lobe ejector/suppressor, it appears that the noise increment and absolute extrapolation technique provide equally favorable estimates of flight noise.

Internal Mixer Results

Tunnel-off and tunnel-on spectra are shown in Fig. 16 for the internal mixer at takeoff power. The near-field 155° spectrum is representative of far-field peak OASPL, which occurs at about 140°. The tunnel-on spectra have been adjusted for Doppler frequency shift and are, therefore, considered to be representative of flight. A reference noise level is included which reflects tunnel-off data at the tunnel-on mixed jet relative velocity ($V_{mix} - V_\infty$). The tunnel-on spectra indicate that mixed jet relative velocity will provide a good flight noise estimate in the region of peak noise.

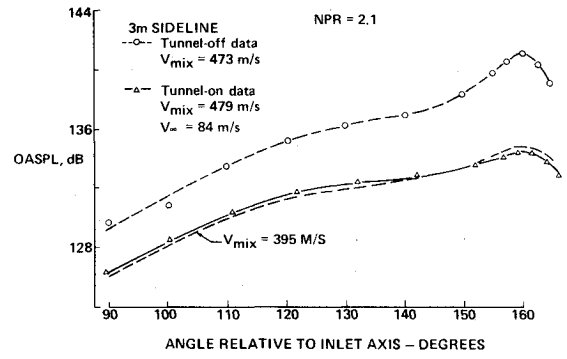

Fig. 17 JT8D-17 engine, internal mixer flight OASPL directivity.

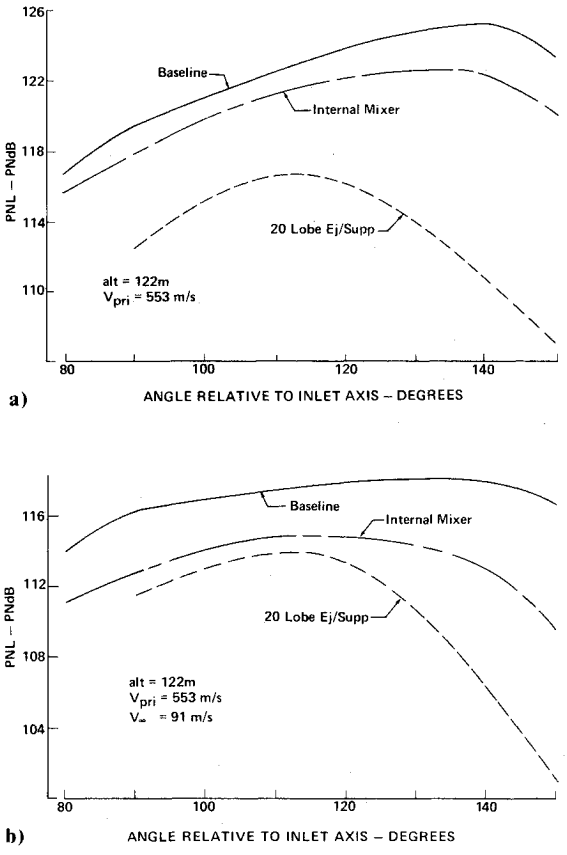

Fig. 18 JT8D engine, a) static and b) flight PNL directivity.

Tunnel-off and tunnel-on OASPL directivities are compared in Fig. 17 for takeoff power. The plot shows that the tunnel-on noise level is predicted closely by the tunnel-off data at equal mixed jet relative velocity over the test range of near-field angles. The location of peak OASPL is changed little due to tunnel velocity. Substantial reduction is shown at all angles, with larger reduction occurring near the region of peak noise.

Comparison of Baseline and Suppressor Static and Flight PNL

A comparison of static and flight PNL directivities is provided in Fig. 18 for the baseline, internal mixer, and 20-lobe ejector/suppressor configurations. The comparisons are made for takeoff power and reflect noise levels for a 727 aircraft during a level flyover at an altitude of 122 m (400 ft). The static PNL estimates are based on far-field data that are extrapolated to the flight condition. The flight noise levels were estimated by subtracting measured wind-tunnel static-to-flight PNL increments from the reference static PNL values.

The PNL directivity comparisons of Fig. 18 emphasize the importance of flight effects to a proper evaluation of a suppressor concept. In going from static to flight operation, the noise characteristics of the internal mixer impove slightly relative to the baseline. That is, the flight PNL suppression is greater than static suppression over the range of angles shown. The 20-lobe ejector/suppressor experiences a significant loss of PNL suppression during flight. Although the ejector/suppressor generates substantially less noise than the internal mixer under static conditions, the in-flight noise levels are much more comparable, in particular at low and peak noise angles. The ejector/suppressor flight PNL at angles near the jet axis is significantly lower than the internal mixer and results in a definite benefit in terms of effective perceived noise level (EPNL).

Conclusions

The following conclusions are made as a result of the JT8D engine noise test in the NASA ARC 40 × 80 ft wind tunnel:

1) Comparisons of 40 × 80 ft wind tunnel and 727/JT8D flight-test OASPL for the baseline and quiet-nacelle configurations show good agreement. Model results obtained in the Boeing 9 × 9 ft wind tunnel for these configurations compare favorably with full-scale wind-tunnel results.

2) Flight-test and wind-tunnel data comparisons indicate that a wind tunnel is a viable method for studying flight effects on jet noise. This flight simulation technique offers great potential for cost savings and development of quiet engine systems that are designed effectively for the flight environment.

3) Measurement of jet noise relatively near to the sources will provide a satisfactory assessment of far-field flight effects if the correlations described herein are applied.

4) The wind-tunnel test shows the importance of testing suppressor concepts for flight noise. The 20-lobe ejector/suppressor experiences a significant loss of suppression during flight, whereas the internal mixer indicates a slight gain in suppression.

References

[1] Strout, F.G., "Flight Effects on Noise Generated by the JT8D-17 Engine in a Quiet Nacelle and a Conventional Nacelle as Measured in the NASA Ames 40- by 80-Ft. Wind Tunnel," NASA CR-137797.

[2] MacGregor, G.R. and Simcox, C.D., "The Location of Acoustic Sources in Jet Flows by Means of the Wall Isolation Technique," *Progress in Astronautics and Aeronautics*, Vol. 38, edited by H.T. Nagamatsu, American Institute of Aeronautics and Astronautics, New York, 1975, p. 431-450.

[3] Hiatt, D.L. and McKaig, M.B., "727 Noise Retrofit Feasibility, Vol. III: Upper Goal Flight Testing and Program Summary," Federal Aviation Agency, FAA-RD-72-40, III, June 1973.